

## 8. Status and features of BigRIPS separator project

### Abstract:

The superconducting in-flight radioactive-isotope (RI) beam separator BigRIPS is being built for the RI-beam factory project at RIKEN. The BigRIPS separator is characterized by large acceptances and a two-stage separator scheme, which can enlarge the scope of RI-beam experiments significantly. The large acceptances allow one to produce RI beams efficiently by using in-flight fission of uranium beams, while the two-stage separator scheme allows one to deliver tagged RI beam. The BigRIPS separator is followed by RI-beam delivery line which transports RI beams to experimental setups placed downstream. The delivery line has been designed to serve as a zero-degree forward spectrometer (ZDS), which is employed to analyze projectile residues in secondary reaction studies of unstable nuclei. A beam dump and a rotating production-target system are being developed and designed for the BigRIPS separator to cope with high-power primary heavy ion beams. Beam-line detectors have been also developed for the RI-beam tagging with high counting rates.

The completion of the BigRIPS separator and the ZDS spectrometer is scheduled in late 2006 and in March, 2007, respectively. The first RI-beam experiment is scheduled in 2007.

In this report, design features and present status of the whole system are outlined.

List of collaborators;

T. Kubo, K. Kusaka, K. Yoshida, A. Yoshida, T. Ohnishi, N. Fukuda, M. Ohtake, Y. Yanagisawa, T. Motobayashi, H. Sakurai and Y. Yano,

Spokesman:

T. Kubo ([kubo@rarfaxp.riken.jp](mailto:kubo@rarfaxp.riken.jp))

## Contents

1. Introduction
2. Outline of BigRIPS separator
3. Superconducting quadrupoles and cryogenic system
4. Radiation heat loads and radiation damage
5. RI-beam delivery line in 2007 and zero-degree forward spectrometer
6. High-power production target and high-power beam dump
7. Development of beam-line detectors for RI-beam tagging
8. Schedule of construction
9. Summary
10. References

## 1. Introduction

The radioactive-isotope (RI) beam factory (RIBF) project, which is based on the in-flight separation scheme, is in progress at RIKEN. [1] In this project three new cyclotrons are being built as an extension of the existing cyclotron facility. The cascade operation of the cyclotrons can provide a wide range of heavy ion beams, boosting the energies up to 400 MeV/nucleon in the case of relatively light elements ( $A < 40$ ) and 350 MeV/nucleon in the case of heavier elements up to uranium. The maximum beam intensity (goal intensity) is expected to be as high as 1  $\mu\text{A}$  ( $6 \times 10^{12}$  pps) even for very heavy elements such as uranium. Such capability allows one to produce RI beams efficiently by using an in-flight RI beam separator, for which in-flight fission of uranium beams as well as projectile fragmentation are used as production reactions.

An in-flight RI beam separator named BigRIPS [2] is being built for the RIBF project. The BigRIPS separator is characterized by two major features: large acceptances and a two-stage separator scheme. The large acceptances are achieved by the use of superconducting quadrupoles with large apertures. This feature enables efficient RI-beam production, even when the in-flight fission of uranium beams at 350 MeV/nucleon is employed as a production reaction. Fission fragments have large spreads in both angle and momentum in our energy domain. The two-stage separator scheme allows one to deliver tagged RI beams: The first stage of BigRIPS separator serves to produce and separate RI beams, while the second stage serves to identify RI-beam species in an event-by-event mode. The tagged RI beams can be delivered to experimental setups placed downstream. Because the purity of RI beams is expected to be poor at our energies, the scheme will facilitate RI-beam experiments such as secondary reaction studies of unstable nuclei. These features and the capability of RIBF cyclotrons are expected to enlarge the scope of RI-beam experiments significantly, promoting studies on properties and reactions of unstable nuclei further from the stability.

The BigRIPS separator is followed by RI-beam delivery line, which transports the tagged RI-beams to the experimental setups. The delivery lines has been designed to serve as a zero-degree forward spectrometer (ZDS), which will be employed for secondary reaction studies of unstable nuclei.

High-power heavy ion beams are used for the RI-beam production. The maximum beam power is expected to be around 100 kW, corresponding to the case of uranium beams at 350 MeV/nucleon and 1  $\mu$ A. The use of heavy ion beams with such high power requires development of a beam dump as well as a production target that can stand the high heat loads. High-energy neutrons emitted from the target and the beam dump are expected to cause radiation damages to some components of the BigRIPS separator as well as to give large radiation heat loads to the cryogenic system of superconducting quadrupoles. These issues are taken into consideration in the design of BigRIPS separator.

The RI-beam tagging is made at high counting rates such as  $10^6$  Hz. Beam-line detectors, which are paced at BigRIPS focuses, have been developed to cope with the high counting rates.

In this report we outline design features and present status of the BigRIPS separator project. Some detailed description is given in reference 2.

## **2. Outline of BigRIPS separator**

Figure 1-a shows a schematic layout of the BigRIPS separator, which has been designed to be a two-stage RI beam separator. The first stage from the production target to the F2 focus comprises a two-bend achromatic spectrometer, consisting of four superconducting quadrupole triplets (STQ) (STQ1 to STQ4) and two room-temperature dipoles (RTD) with a bending angle of 30 degrees (D1 and D2). This first stage serves to produce and separate RI beams. The in-flight fission of uranium beams as well as the projectile fragmentation of various heavy ion beams are employed as production reactions. An achromatic wedge-shaped degrader is inserted at the momentum-dispersive focus F1 at an intermediate point to make isotopic separation based on the technique called momentum achromat. A high-power beam dump is placed inside of the gap of the first dipole D1 as well as the exit of D1 to stop primary heavy ion beams. The first stage is surrounded by thick concrete blocks, in order to shield neutron radiation from the target and beam dump. A telescopic system consisting of two STQs (STQ5 and STQ6) follows the achromatic focus F2, being used to transport separated RI beams to the second stage. The second stage from the F3 focus to the F7 focus consists of eight STQs (STQ7 to STQ14) and four RTDs with a bending angle of 30

degrees (D3 to D6), comprising a four-bend achromatic spectrometer. The intermediate focuses F4, F5 and F6 are momentum-dispersive, while the final focus F7 is doubly achromatic. Figure 1-b shows a photograph of the BigRIPS hall under construction in 2002, in which the BigRIPS separator is placed.

Since our energy domain is not so high, the purity of RI beams is expected to be poor due to the nature of energy loss as well as the mixture of charge state. RI beams produced are so-called cocktail beams in which several isotopes are mixed. To overcome this difficulty, the second stage of BigRIPS separator is employed to identify RI-beam species. Position-sensitive detectors, timing detectors and  $\Delta E$  detectors are placed at the focuses of the second stage to measure the magnetic rigidity ( $B\rho$ ), the time-of-flight (TOF) and the energy loss ( $\Delta E$ ) of RI beams. The scheme allows one to determine the atomic number ( $Z$ ), the ratio of mass number to charge number ( $A/q$ ) and the momentum ( $P$ ) in an event-by-event mode, making it possible to deliver tagged RI beams to experimental setups placed downstream of the BigRIPS separator. The concept of RI-beam tagging is depicted in Fig. 2. RI-beam experiments, particularly those of secondary reaction studies, are significantly facilitated by the delivery of tagged RI beams.

It is also possible to make two-stage separation by placing another energy degrader at the F5 focus on the second stage.

The angular acceptances of the BigRIPS separator have been designed to be 80 mr horizontally and 100 mr vertically, while the momentum acceptance will be 6 %. The maximum bending power is 9 Tm. The total length is 77 m. The angular and momentum spreads of fission fragments at 350 MeV/nucleon are estimated to be about 100 mr and 10 %, respectively, when symmetric fission is assumed. The acceptances of BigRIPS are comparable to those values, allowing one to achieve high collection efficiency for the in-flight fission: almost half of the produced fission fragments may be accepted for some isotopes. These high acceptances are made possible by the use of superconducting quadrupoles with large apertures and room-temperature dipoles with a large gap. Basic parameters of the BigRIPS separator are listed in Table 1, while its first-order optics is shown Fig. 3.

Fabrication of the quadrupoles and dipoles was complete in March, 2004. Installation of the first-stage magnets (STQ1-5 and D1-2) was also made then, including their cryogenic system. Some photographs taken in 2004 are shown in Fig. 4a-c.

Figure 4-d shows recent photographs of the BigRIPS hall and the second-stage STQs. Installation of the second-stage magnets begins soon in 2005. The completion of BigRIPS separator is scheduled in late 2006.

### **3. Superconducting quadrupoles and cryogenic system**

The quadrupoles of the BigRIPS separator have been designed to be superconducting triplets. Three superconducting quadrupoles are installed in a helium vessel in a single cryostat, being cooled by a liquid-helium bath. Most of the superconducting quadrupoles are of an iron-dominated type, except for those of the quadrupole triplet STQ1 which is placed right after the production target.

All the iron-dominated superconducting quadrupoles have an identical cross section. Their pole-tip radius and warm bore radius are 170 mm and 120 mm, respectively. The maximum pole-tip fields are 2.4 T, corresponding to a field gradient of 14.1 T/m. The nominal effective lengths of the three quadrupoles are 0.5 m, 0.8 or 1.0 m and 0.5 m, respectively. The quadrupole coils are impregnated with epoxy, being orderly wound with a thin NbTi superconducting wire having a diameter of 1.1 mm. They are flat coils with a racetrack shape. The Ampere-turn of the coils is about 200 kA/pole. The cold mass weight of the quadrupole triplet is about 12 tons and the helium vessel stores liquid helium of 600 liters. More details of the iron-dominated STQ are given in references 3 and 4.

The superconducting quadrupole triplet STQ1 has been designed to be of an air-core type, considering the radiation heat loads to the cryostat. A much smaller cold-mass weight of this type reduces the heat load significantly. The quadrupole coils of the air-core type are also flat and of a racetrack shape, being orderly wound with a thicker NbTi superconducting wire with a rectangular cross section. The specifications of STQ1 is as follows: the nominal effective lengths of three quadrupoles are 0.5 m, 0.8 m and 0.5 m, respectively; their warm bore radii are 90 mm, 120 mm and 120 mm, respectively; and their maximum field gradients are 24 T/m, 20 T/m and 20 T/m, respectively. More details are given in reference 5.

Figure 5 shows some photographs of the STQs taken in a Toshiba factory.

The five quadrupole triplets in the concrete shielding (STQ1 to STQ5) are cooled by

an integrated, large-scale cryogenic system with a large cooling capacity, in which a single refrigerator supplies liquid helium to their cryostats through a transfer line (about 50 m long). [6] Figure 6 shows its schematic diagram. The cooling capacity of the refrigerator has been measured to be about 510 W for refrigeration at 4.5 K. It should be more if liquid nitrogen is supplied to the refrigerator. This scheme has been chosen considering the radiation heat loads to the cryogenic system.

On the other hand, the quadrupole triplets downstream (STQ6 to STQ14) are cooled by a small refrigeration system in which a GM-JT refrigerator is employed. [4] The small refrigeration system is mounted on the cryostat of each quadrupole triplet. Figure 7 shows its schematic drawings. The cooling capacity of the refrigerator is as small as about 2.5 W at 4.3 K. The refrigerator just re-liquefies evaporating liquid helium. To make the refrigerator operational, it is necessary to pre-cool the cold mass using liquid nitrogen and liquid helium. We chose this scheme considering the fabrication cost.

A gas-cooled current lead with multiple electrodes is employed for the first five quadrupole triplets (STQ1-5). Five current leads in each cryostat are installed in a single cooling-gas channel, with which no complicated multi-channel gas-flow control is needed. More details are given in reference 7. On the other hand, for the STQs with a small refrigeration system (STQ6-15), high-Tc superconducting current leads are used to reduce heat loads. [4]

#### **4. Radiation heat loads and radiation damage**

The superconducting quadrupole triplets in the first stage of BigRIPS (STQ1 to STQ5), particularly the first two triplets STQ1 and STQ2, are exposed to neutron radiation from the production target and the beam dump, which gives significant heat loads to their cold mass at 4.5 K in the cryostats. The normal heat loads to the whole cryogenic system have been measured to be about 210 W at 4.5 K: 100 W for the transfer line, 20 W for the five STQs and 90 W for the cooling of current leads. Hence the cooling capacity of about 300 W can be used for the radiation heat loads.

The radiation heat loads change depending on the operating condition of the BigRIPS separator as well as the intensity of the primary heavy ion beams. For instance they suddenly disappear when primary beams are switched off. Heaters installed in the quadrupole cryostats are employed to compensate those changes, allowing stable

operation of the cryogenic system.

The neutron radiation from the production target and the beam dump are expected to radiation damage some nearby components in the first stage of the BigRIPS separator. It is technically impossible for us to overcome this problem by using radiation-resistant materials for all the components. Instead, we tried to avoid using radiation sensitive materials, so that the components can survive as long as possible. We checked materials of almost all the components and chose the least sensitive ones that are currently available. For instance, in the case of the superconducting quadrupoles, polyimide (Kapton) coating is employed for insulation of the NbTi wire, and superinsulation made of a polyimide foil is used in the cryostats. Radiation-resistant materials are used in some cases if they are available. For instance full mineral insulated coils are used for the first dipole where the beam dump is placed. For some components such as a valve box of the cryogenic system, local radiation shielding is used to reduce damage.

The superconducting quadrupoles STQ1 and STQ2 may be destroyed in a few years. We plan to just replace them by new ones when it happens. The BigRIPS separator is being so designed that the replacement can be made easily under the condition with high residual radiation.

## **5. RI-beam delivery line in 2007 and zero-degree forward spectrometer**

Figure 8 shows a schematic layout of the RI-beam delivery line in 2007, along with the BigRIPS separator. It is placed in the experimental hall, transporting RI-beams to experimental setups placed downstream. The same dipoles and the same STQs with the small refrigeration system as those of the BigRIPS separator are used for the magnets of delivery line. Fabrication of the delivery-line magnets has started in 2005.

As shown in Fig. 8, the delivery line has been designed to serve as a zero-degree forward spectrometer (ZDS) by which projectile residues (ejectiles) from secondary reactions of RI beams are analyzed and identified. Figure 9 schematically shows a schematic layout of the ZDS spectrometer. It consists of six STQs and two dipoles, being designed to be an anti-mirror achromatic system with two intermediate focuses. The intermediate focuses are momentum dispersive, while the final one is achromatic. In this achromatic mode, the first-order momentum resolution at the intermediate focuses is about 1200 when the acceptances similar to those of BigRIPS are achieved.

It is possible to increase the resolution to some extent by tuning the optics, although the acceptances are reduced. In addition to the achromatic mode, it is possible to operate the ZDS spectrometer in a dispersive mode to get a high momentum resolution. A momentum resolution of about 4000 can be achieved. In this mode an intermediate focus is located at the mid-point of the system and the final focus is momentum dispersive. More details are given in reference 8. The operation mode of ZDS spectrometer can be selected depending on the experimental conditions.

Reaction and structure studies of unstable nuclei are to be carried out by using the ZDS spectrometer. One of the main subjects is in-beam  $\gamma$  ray spectroscopy of unstable nuclei by using secondary reactions of RI beams, such as light-ion reactions in inverse kinematics, *e.g.* (p,p'), ( $\alpha,\alpha'$ ), (d,p), ( $\alpha,t$ ) etc., and intermediate-energy Coulomb excitation. In this case the ZDS is employed to identify projectile residues of the secondary reactions in coincidence with  $\gamma$  rays from the projectile-residue nuclei. For the  $\gamma$ -ray measurement,  $\gamma$ -ray array detectors, such as NaI and Ge arrays, are placed so as to surround the secondary target.

According to a long flight path and a medium momentum resolution of the ZDS, a nice resolving power in the particle identification can be achieved even for a heavy mass region up to  $A=200$ .

The construction of the delivery-line will be complete in March, 2007.

## **6. High-power production target and high-power beam dump**

The beam power expected in the RIBF is quite high. It is around 100 kW at maximum: *e.g.* 45 kW for  $^{136}\text{Xe}$  and 84 kW for  $^{238}\text{U}$  at 350 MeV/nucleon and 1  $\mu\text{A}$ . To cope with such a high heat load, we are developing and designing a high-power production target [9,10] and a high-power beam dump [11,12], both of which are cooled by water flow.

The beam power deposited in the production target is expected to be around 25 kW at maximum and the beam size on target is expected to be 1 mm in diameter. This corresponds to the power density of about 30 GW/m<sup>2</sup> and to the volume power density of 5.7 kW/mm<sup>3</sup> in the case of carbon target. A water-cooled rotating disk target system is being developed to cope with such a high power density. Figure 10 shows its schematic drawing. A disk-shaped production target is mounted on a water-cooled

rotating disk, for which the cooling water is supplied through a rotating shaft. Simulation studies as well as beam testing have shown that this target system can stand the expected heat load. [9,10]

Figure 11 shows a schematic drawing of the target system for BigRIPS, which is being designed. A part of a mockup for the system, as shown in the photograph of Fig. 11, was constructed and has been tested in off-line. [13] Radiation hardness of magnetic fluid used for a vacuum seal of the rotating shaft has been tested up to the total dose of 0.5-1.5MGy and no significant change on its viscosity was found. [14]

Primary beams stop at the first dipole magnet (D1) of the BigRIPS separator, the stopping position being dependent on the operational conditions. Figure 12 shows trajectories of primary beams for several different  $B\rho$  settings. When the  $B\rho$  value of primary beams is far from that of RI beams, the primary beams stop on either right or left hand sides of the D1 dipole, depending on whether the RI beams are proton-rich or neutron-rich. This mostly happens when RI beams are produced by projectile fragmentation. When neutron-rich RI beams are produced by in-flight fission of neutron-rich uranium beams, the primary beams do not always stop at the side of the D1 dipole, but come out of the dipole. Hence the beam dump is placed not only on both sides of the vacuum chamber of the D1 dipole, but also at the exit of the dipole. We call them the side-wall beam dump and the exit beam dump, respectively.

The BigRIPS beam dump that we are designing is water-cooled one for which a swirl tube and a screw tube are employed. Figure 13 shows schematic diagrams of the tubes through which pressurized cooling-water flows. The use of such tubes significantly improves the heat transfer coefficient of water flow [15], so that the temperature of beam dump can be reduced.

Figures 14 shows schematic drawings of the BigRIPS beam dump being designed. In order to reduce the temperature, the shape and geometry of the beam dump has been so arranged that the projected heat density on the beam-dump surface can be significantly reduced. The side-wall beam dump looks like a tilted-V shaped wall, being placed along the bending curvature of the dipole. This geometry enlarges the projected beam-spot size significantly. Figure 15 shows a schematic diagram of the side-wall beam dump. It consists of many copper-alloy swirl tubes having rectangular cross sectional shape. The swirl tube has a twisted ribbon along the inside, so that the heat transfer coefficient can be improved. The water flow is in mixed phase, in other

words, in subcooled boiling phase in which it contains locally boiling water. The heat is removed by not only forced convection but also latent heat of evaporation of water. The water flow is pressurized to obtain a temperature margin since the boiling point of water increases with pressure.

Figure 16 shows a schematic drawing of the exit beam dump. It looks like a tilted-V shaped beam stopper and moves in the horizontal direction. The position is adjusted according to the primary-beam trajectory. In the case of exit beam dump the screw tube is employed for the water-cooling to improve the heat transfer further.

The size and shape of beam spot at the beam dump changes depending on where the beam stops. So does the power density on the surface of beam dump. If the beams are injected perpendicularly to the beam dump wall, the power density amounts to several hundreds  $\text{MW}/\text{m}^2$  in the worst case, which causes critical damages to the beam dump. However the power density can be reduced down to a few tens  $\text{MW}/\text{m}^2$ , because the projected beam-spot size is magnified due to the small injection angles with respect to the beam-dump wall and the vertically tilted wall. Simulation studies have shown that it is possible to build a beam dump that can withstand the expected beam power density.

## **7. Development of beam-line detectors for RI-beam tagging**

The delivery of tagged RI beams facilitates RI-beam experiments significantly, since the RI beams produced are expected to be of cocktail beams. The RI-beam tagging is made by the event-by-event particle identification using the  $B\rho$ - $\Delta E$ -TOF method, which allows one to determine the atomic number ( $Z$ ), the ratio of mass number to charge number ( $A/q$ ) and the momentum ( $P$ ) of RI-beam species. Furthermore, the particle-tracking method is employed in order to determine the  $B\rho$  and TOF values more precisely. Position detectors such as parallel-plate avalanche counters (PPAC) [16,17],  $\Delta E$  detectors such as ionization gas chambers [18], and timing detectors such as thin plastic scintillation counters are placed at the focuses of BigRIPS separator to measure the  $B\rho$  value, the energy loss, and the time-of-flight, respectively. Those beam-line detectors are required to work well at counting rates up to  $10^6$  Hz and to have a relatively large active area.

A delay line parallel-plate avalanche counter (DL-PPAC) has been developed in order

to measure the position of RI beams with high detection efficiency at high counting rate around  $10^6$  Hz. [16,17] Owing to its simple structure, the radiation hardness and the simple readout system are the characteristics of DL-PPAC. This counter has been already used for a long time at RIPS separator [19], and has been proven to be very versatile and reliable. The performance of DL-PPAC for high-Z particles at higher energies was tested by using  $^{132}\text{Xe}$  beam at 400 MeV/nucleon at HIMAC facility [20]. The position resolution has been measured to be  $\sigma = 0.5$  mm, which is good enough to determine the Bp value with the resolution better than  $10^{-3}$  at BigRIPS. The active area of DL-PPAC has been enlarged from  $100 \times 100$  mm<sup>2</sup> to  $240 \times 150$  mm<sup>2</sup>, since the larger size is needed for BigRIPS. The large-area DL-PPAC did not show any position dependence of the resolution in the test measurement.

For the energy loss measurement at the high counting rates, a tilted-electrode gas ionization chamber (TEGIC) has been developed. [18] Although the basic idea of TEGIC is almost the same as MUSIC at GSI [21], the structure of electrodes is very different. A total of 24 grid-less parallel ionization chambers, of which anode and cathode electrodes are made of thin foils, are stacked together back to back, and incident particles pass through all of those parallel ionization chambers (including the electrode foils). The electrode planes are tilted by 30 degrees toward the beam axis in order to avoid the recombination of electrons and positive ions liberated from the gas along the particle trajectories. The gaps between the anode and cathode foils are as small as 20 mm. As a result of the structure, a large active area is made possible, and a short drift time can be achieved, allowing a high counting rate measurement. Furthermore, the spread of drift time becomes small, because the drift length does not much depend on incident particle trajectories. The prototype of TEGIC detector was tested by using  $^{132}\text{Xe}$  beams at 400 MeV/nucleon at HIMAC, and the measured energy resolution was found sufficient to tag RI beams around  $Z = 50$ . The TEGIC with active area of 200 mm in diameter has been also tested at RIKEN [22]. The energy resolution was the same as the prototype one and did not depend on the incident position. To handle rates up to  $10^6$  Hz, the development of amplifier system is underway.

Signal transport system using an optical-fiber cable is the highlight of the readout system of the BigRIPS beam-line detectors. Electrical signals from the detectors are converted to light signals by using a laser diode, and the light signals are transported

through an optical-fiber cable, keeping amplitude and timing information. The transport loss is quite small in this scheme. At the end, the signal is restored to its original shape by using a photo diode. This signal transport system has several merits: analog signals from the detectors can be transported a long distance to a counting room; the electric ground of the detectors can be isolated from that of counting room; and it is easy to add a long delay time ( $> 100$  ns) to signal line without pulse distortion. The delay line using the optical-fiber cable needs small space.

Data acquisition system (DAQ) for BigRIPS is based on the conventional scheme in which a common trigger signal is used. All the signals needed to make the trigger signal are transported from the focuses to the counting room by the optical-fiber cable. For data handling system, it is planned to use CAMAC modules, because the total number of signals at a time is not so much, and the assets of CAMAC module can be applied. To combine the BigRIPS DAQ system with that of experimental setups, we plan to use a new CAMAC crate controller, CC/NET, which was developed at KEK [23] to distribute a data through network. By using this controller, it is easy to combine with other DAQ systems of various experiments.

## **8. Schedule of construction**

Construction and some detailed design of the BigRIPS separator and the RI-beam delivery line are in progress. Figure 17 summarizes the construction schedule. The first RI-beam production using BigRIPS only is scheduled in late 2006, while the first RI-beam experiments will start in early 2007.

An additional budget of 200M yen is needed to perform experiments with the ZDS spectrometer. The budget will be used for beam-line detector system, electronics modules including DAQ system, secondary-target equipment and so on.

## **9. Summary**

In summary the design features and present status of the BigRIPS separator project are outlined. The BigRIPS separator is a next-generation separator with upgraded features, being characterized by large acceptances and a two-stage separator scheme. The integrated capability of the BigRIPS separator and the RIBF cyclotrons will

promote future RI-beam experiments.

## 10. References

**The references [4-9], [10-15] and [17-18] are attached in the appendix.**

- [1] Y. Yano, *Proc. 17th Int. Conf. on Cyclotrons and their Applications*, Tokyo Japan, October 18-22, 2004, ed. A. Goto and Y. Yano, Particle Accelerator Society of Japan, p. 169 (2005).
- [2] T. Kubo, *Nucl. Instr. and Meth.*, **B 204**, 97 (2003).
- [3] T. Hiramachi et al., *IEEE Trans. Appl. Supercond.*, **10**, 236 (2000).
- [4] K. Kusaka et al., *IEEE Trans. Appl. Supercond.*, **14**, 310 (2004).
- [5] K. Kusaka et al., *RIKEN Accel. Prog. Rep.*, **37**, 297 (2004).
- [6] T. Kubo et al., *RIKEN Accel. Prog. Rep.*, **36**, 316 (2003).
- [7] N. Kakutani et al., *RIKEN Accel. Prog. Rep.*, **37**, 299 (2004).
- [8] Y. Mizoi et al., *RIKEN Accel. Prog. Rep.*, **38**, 297 (2005).
- [9] A. Yoshida et al., *Nucl. Instr. and Meth.*, **A 521**, 65 (2004).
- [10] A. Yoshida et al., *RIKEN Accel. Prog. Rep.*, **37**, 295 (2004).
- [11] Y. Mizoi et al., *RIKEN Accel. Prog. Rep.*, **36**, 318 (2003).
- [12] Y. Mizoi et al., *RIKEN Accel. Prog. Rep.*, **38**, 295 (2005).
- [13] A. Yoshida et al., *RIKEN Accel. Prog. Rep.*, **38**, 296 (2005).
- [14] A. Yoshida et al., *Research Report of Laboratory of Nuclear Science, Tohoku University*, **36**, 111-114 (2003).
- [15] J. Boscary et al., *Fusion Engineering and Design*, **43**, 147 (1998).
- [16] H. Kumagai et al., *RIKEN Accel. Prog. Rep.*, **31**, 164 (1998).
- [17] H. Kumagai et al., *Nucl. Instr. and Meth.*, **A470**, 562 (2001).
- [18] K. Kimura et al., *Nucl. Instr. and Meth.*, **A538**, 608 (2005).
- [19] T. Kubo et al., *Nucl. Instr. and Meth.*, **B70**, 309 (1992).
- [20] Y. Hirano et al., *Nucl. Phys.*, **A538**, 541c (1992).
- [21] A. Stolz, et al., *GSI Scientific Report 1998*, 174.
- [22] K. Sugawara et al., *RIKEN Accel. Prog. Rep.*, **37**, 159 (2004).
- [23] KEK online group, <http://www-online.kek.jp/~yasu/Parallel-CAMAC/>.

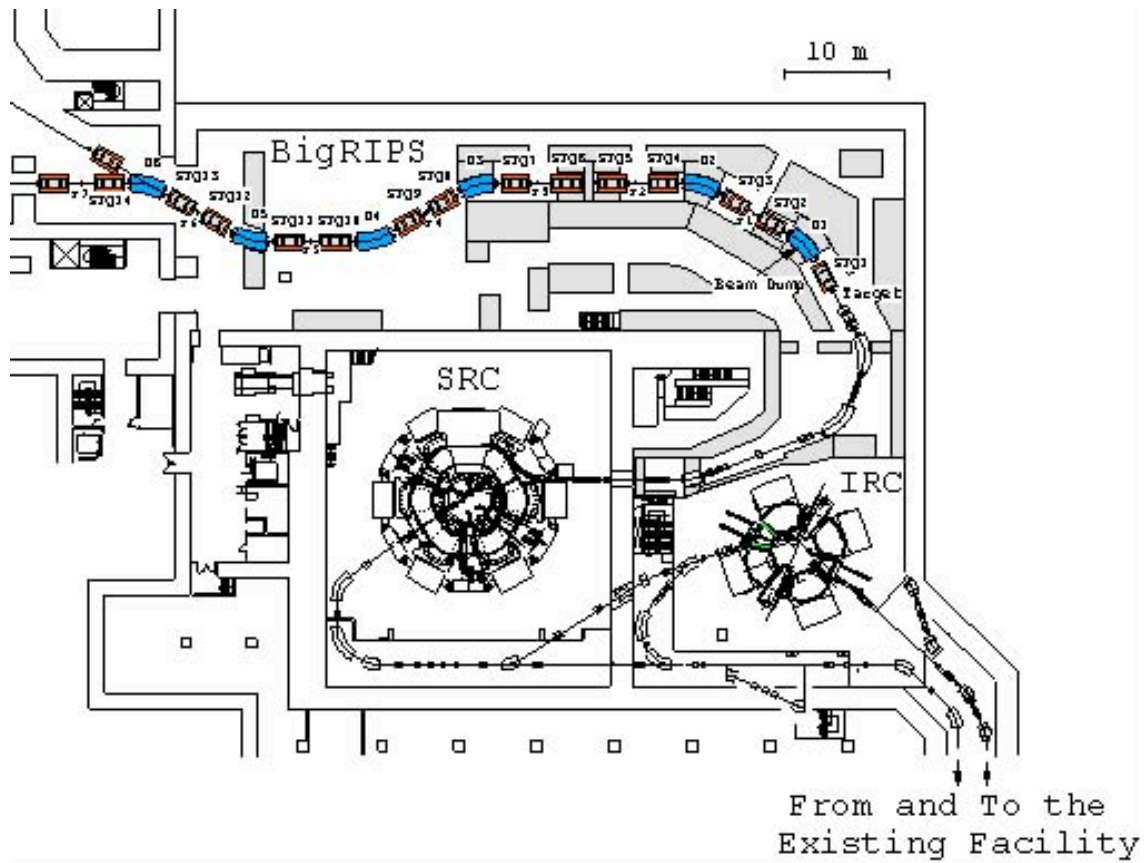


Fig. 1-a. A schematic layout of the BigRIPS superconducting fragment separator at RIKEN. The superconducting quadrupole triplets are indicated by STQ<sub>n</sub>, while the dipole magnets (room temperature) are indicated by D<sub>n</sub>. F<sub>n</sub> denote focuses. IRC and SRC indicate the cyclotrons being built in the RIBF project.



Fig. 1-b. A photograph of the BigRIPS hall taken in February, 2002.

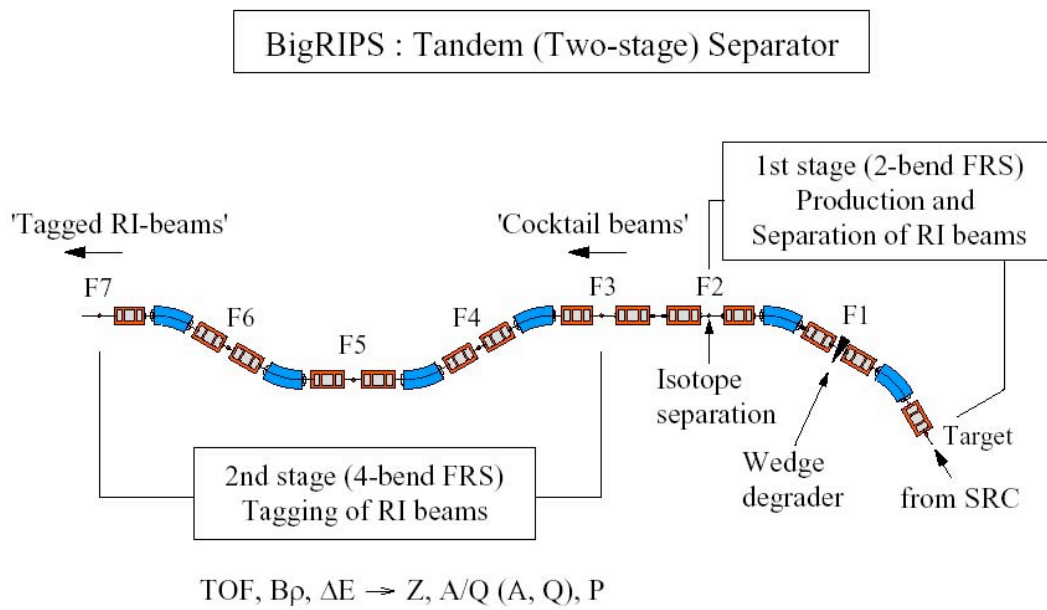


Fig. 2. A schematic diagram of the RI-beam tagging in the BigRIPS separator.

Table 1. Basic parameters\* of BigRIPS separator

Configuration	Two-stage separator
First stage	Two bends
Second stage	Four bends
Energy degrader	Achromatic wedge
Quadrupoles	Superconducting
Angular acceptance	
Horizontal	80 mr
Vertical	100 mr
Momentum acceptance	6 %
Max. magnetic rigidity	9 Tm
Total length	77 m
Momentum dispersion**	
First stage	-2.31 m
Second stage	3.3 m
Momentum resolution***	
First stage	1290
Second stage****	3300

\* Standard parameters.

\*\* At the mid-focus of the stage.

\*\*\* Those in the case that a 1 mm beam-spot is assumed.

\*\*\*\* It is possible to operate the second stage in a full dispersive mode to increase much the momentum resolution. The F7 focus is momentum-dispersive in this case.

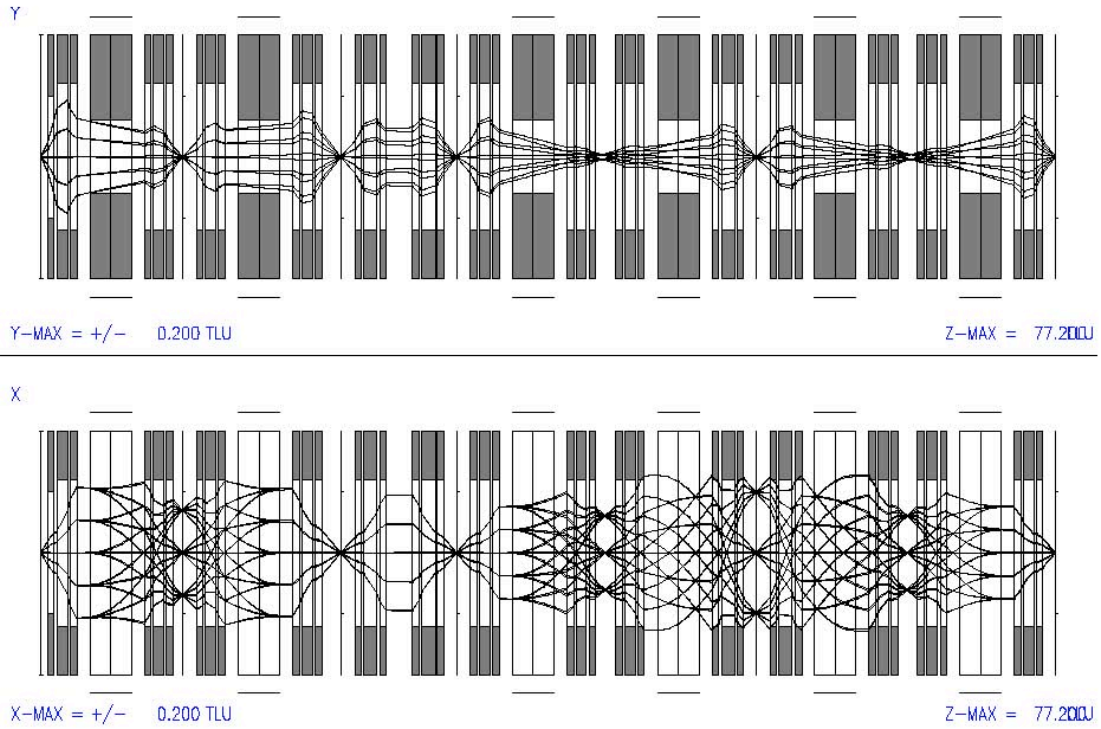


Fig. 3. The first-order optics of BigRIPS separator. The upper figure shows the vertical direction, while the lower one the horizontal direction.

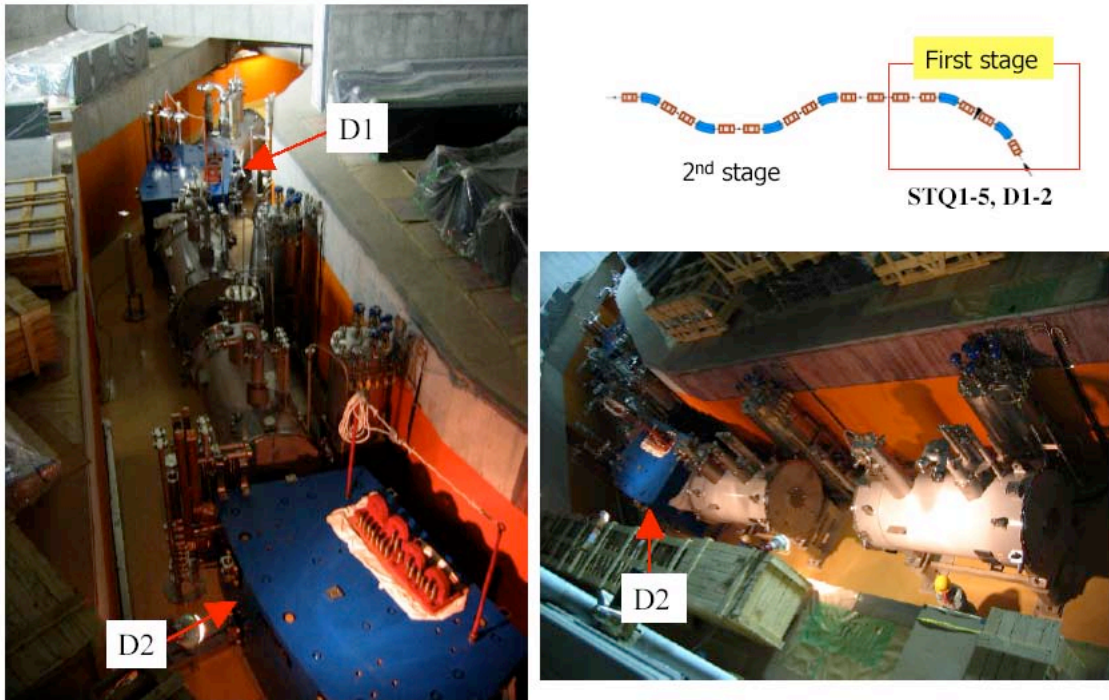


Fig. 4-a. Photographs of the BigRIPS first stage of which magnets have been installed.



Fig. 4-b. Photographs of the cryogenic system for the first-stage quadrupoles.



STQ6-14



D3-6

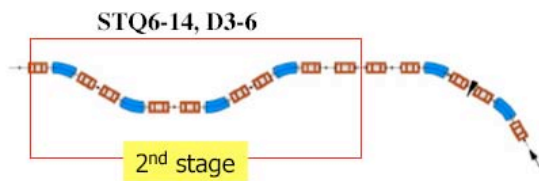


Fig. 4-c. Photographs of the BigRIPS hall and the second-stage magnets: STQ6 to STQ14 and D3 to D6. The magnets will be installed in 2005.



Fig. 4-d. Recent photographs of the BigRIPS hall and the second-stage STQs.



Superconducting quadrupole triplet(STQ):  
Warm bore radius= 12 cm, 12 ton

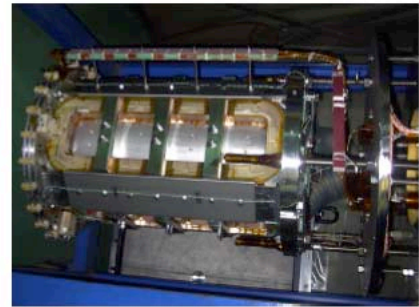


30-degree bend R.T. dipole:  
gap=14 cm,  $\rho=6$  m, 60 ton



Superconducting  
coils

Iron-dominated  
quadrupole



Air-core type quadrupole

Fig. 5. Some photographs of the BigRIPS magnets taken in a Toshiba factory.

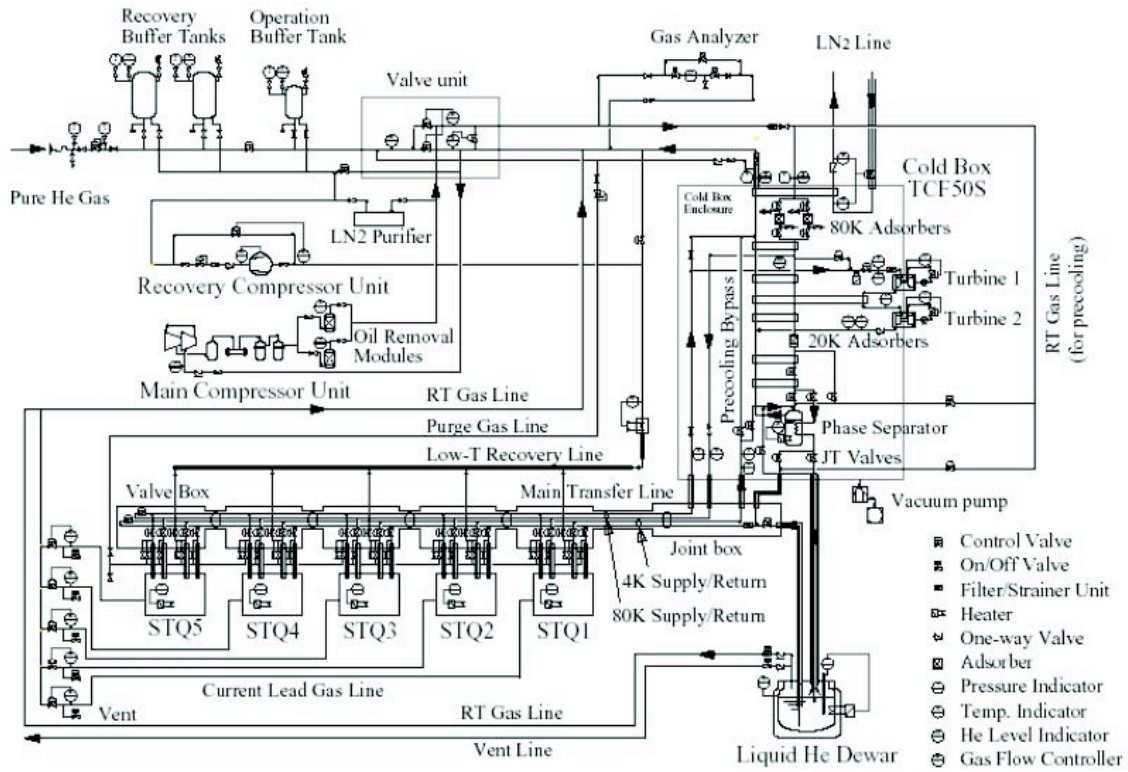


Fig. 6. A schematic diagram of the cryogenic system for the first five quadrupole triplets: STQ1 to STQ5. The Linde TCF50S is employed as a refrigerator.

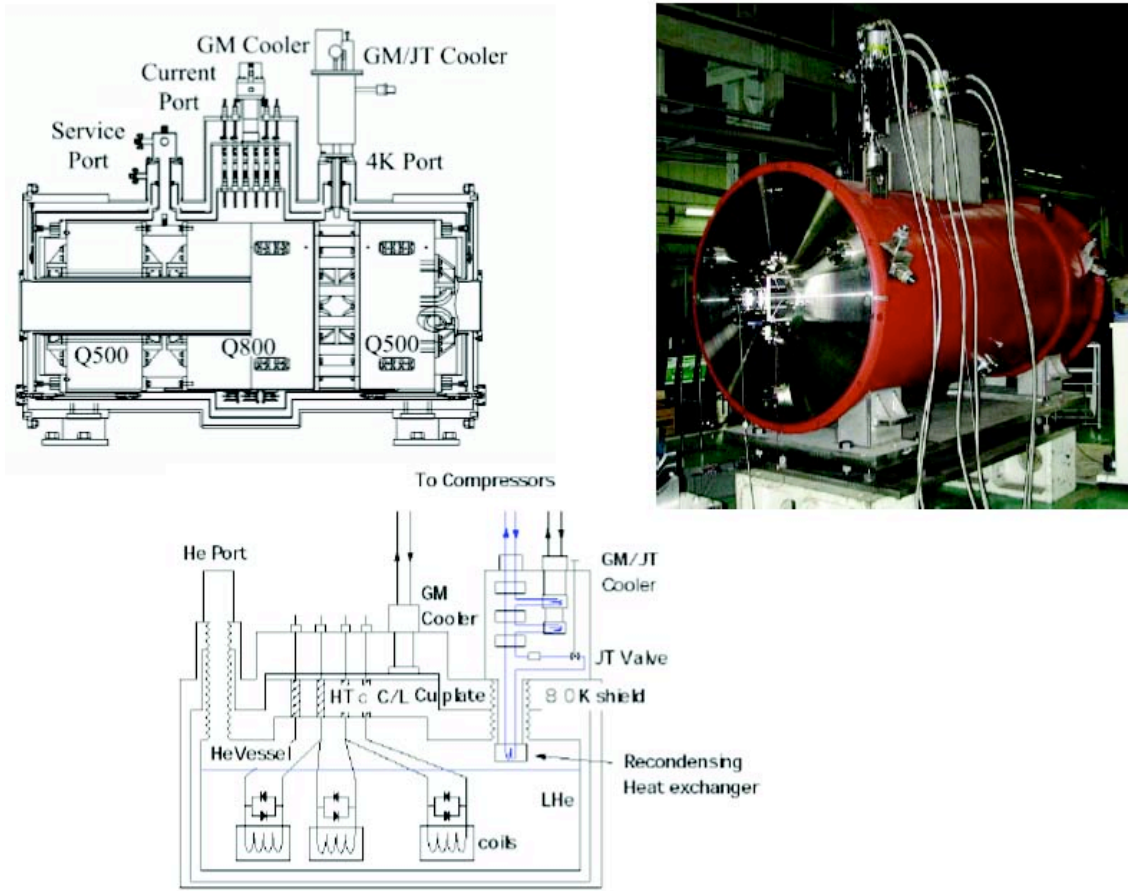


Fig. 7. Schematic diagrams of the quadrupole triplet cooled by a small GM/JT refrigerator: STQ6 to STQ14. The photograph shows a prototype built in 2002.

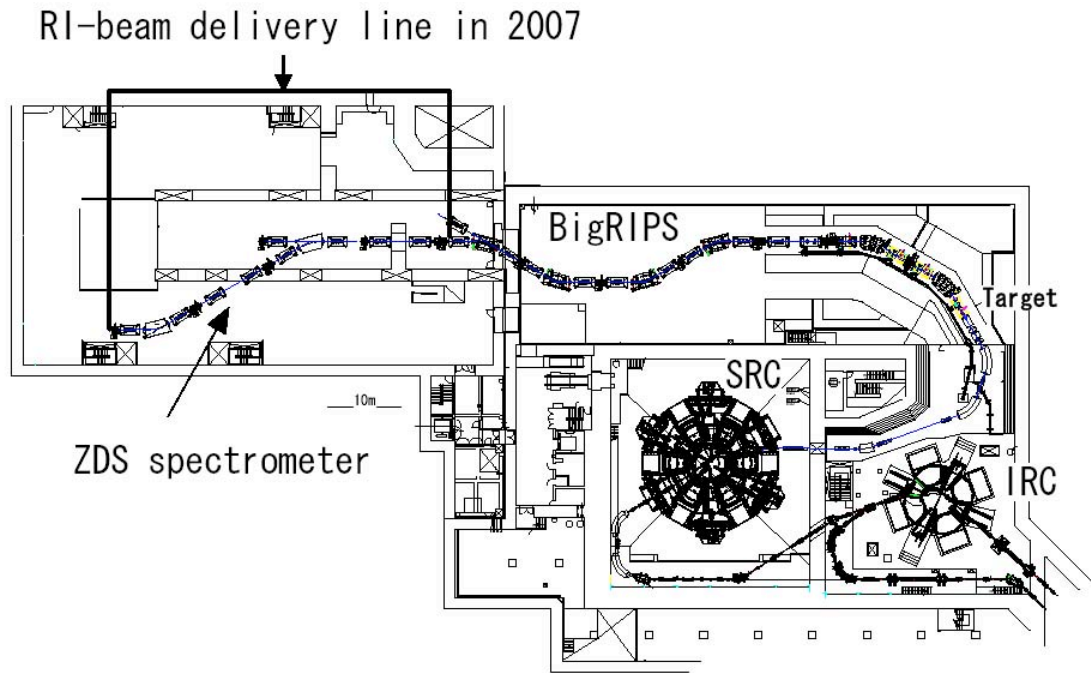


Fig. 8. A schematic layout of the RI-beam delivery line in 2007. Part of the line serves to be a zero-degree recoil spectrometer (ZDS).

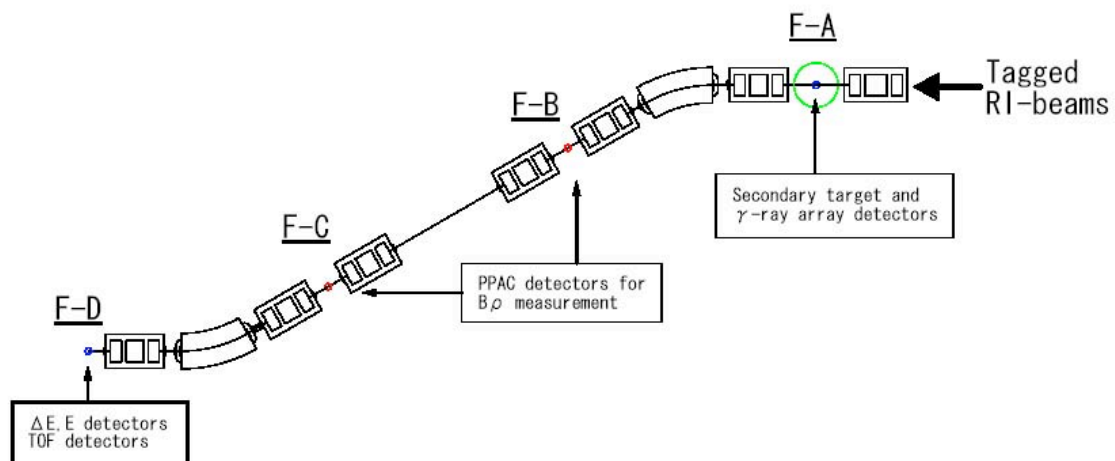


Fig. 9. A schematic diagram of the ZDS spectrometer. F-A to F-D denotes focuses.

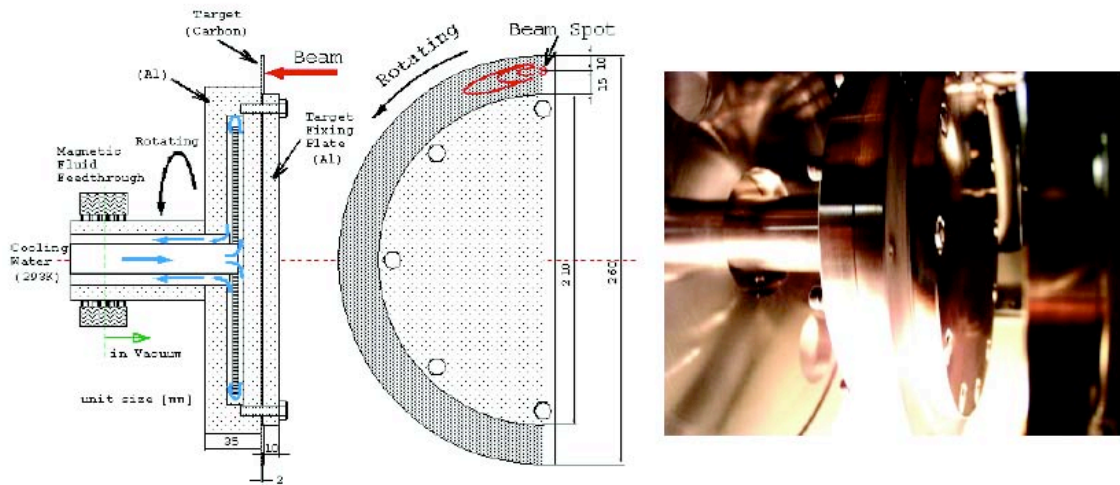


Fig. 10. A schematic drawing of the water-cooled rotating disk target (left) is shown along with a photograph of a prototype.

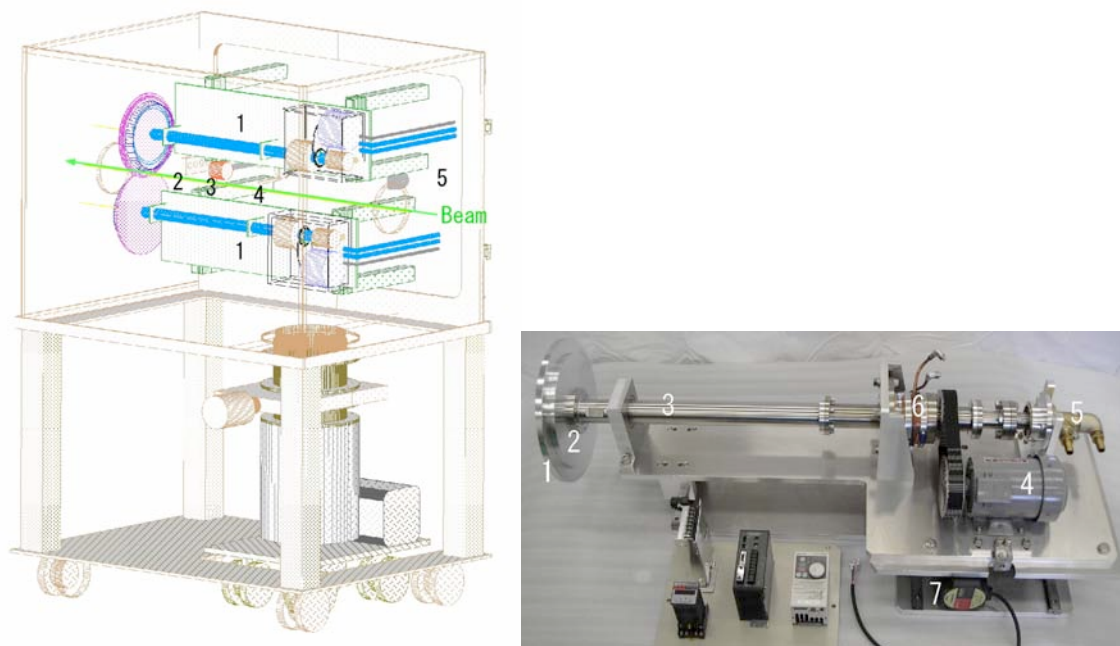


Fig. 11. A conceptual design of the BigRIPS target chamber (left). Two sets of rotating target mechanics (1), a beam viewer (2), a Faraday cup (3) and a beam profile monitor (4) are planned to be mounted on one vacuum flange (5). A mockup of the target system (right). A target wheel (1) and a water-cooled disk (2) connected to a double-piped shaft (3) were rotated using a motor (4). The motor, a rotary joint (5) and a ferromagnetic feedthrough (6) are placed in a small vacuum tight box. All the target mechanics can slide perpendicular to the beam axis using a vacuum motor (7).

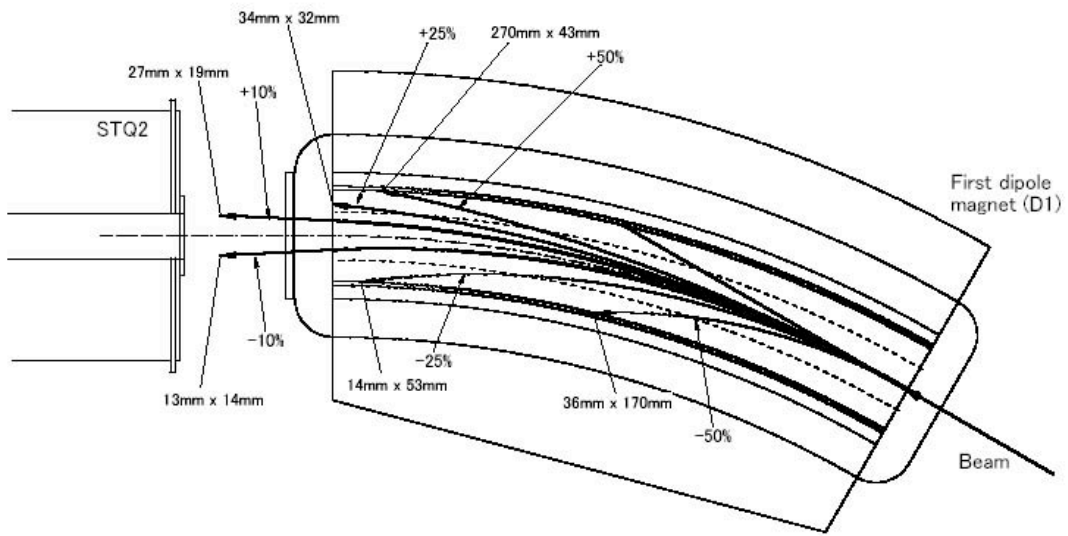


Fig. 12. Trajectories and beam-spot size of primary beams for several different Br settings.

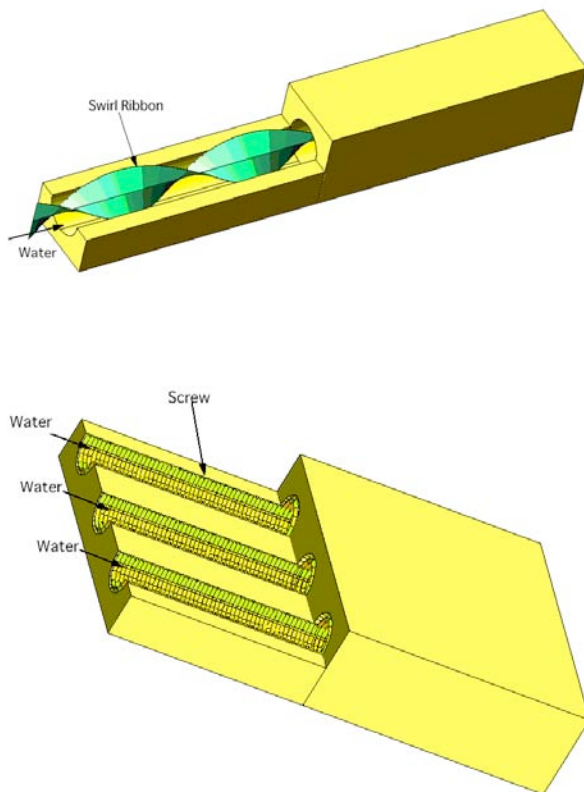
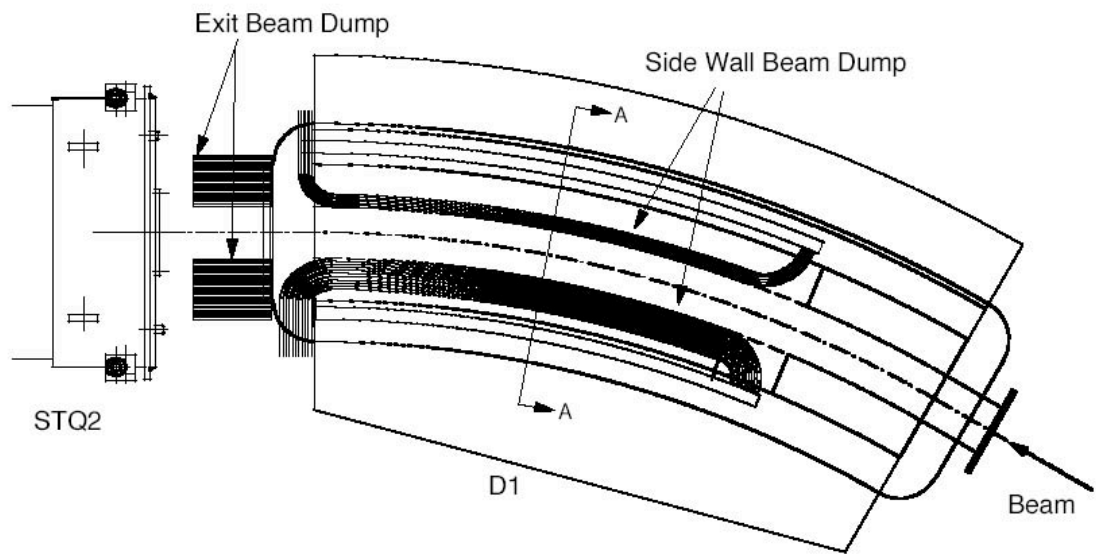


Fig. 13. Schematic diagrams of the swirl tube (upper) and screw tube (lower), which are employed to water-cool the BigRIPS beam dumps. They are made of copper alloy.



Cross-sectional view of the beam dump at A-A

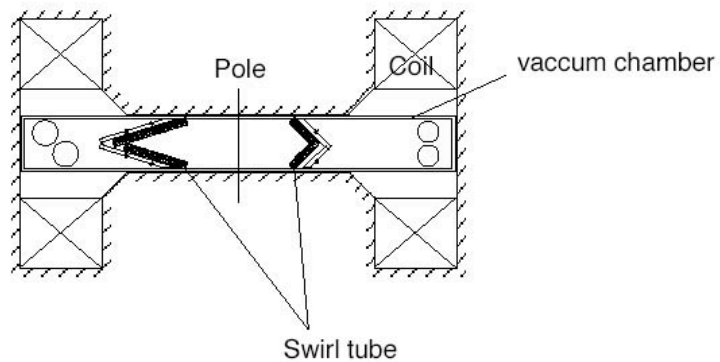


Fig. 14. Schematic drawings of the BigRIPS beam dumps placed at the first dipole magnet: the side-wall beam dump and the exit beam dump. They are water-cooled by using a swirl tube and a screw tube, respectively, through which pressurized water flows.

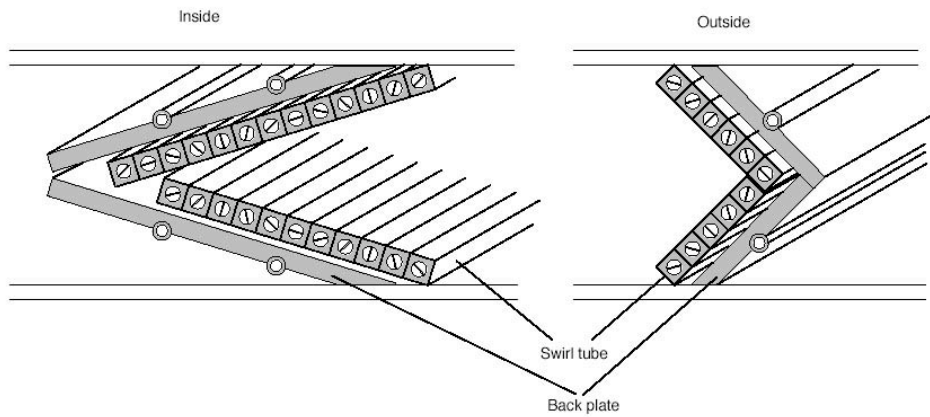


Fig. 15. A schematic diagram of the side-wall beam dump which consists of the copper-alloy swirl tubes with rectangular cross-sectional shape. The beams stop at a small depth of the tube surface.

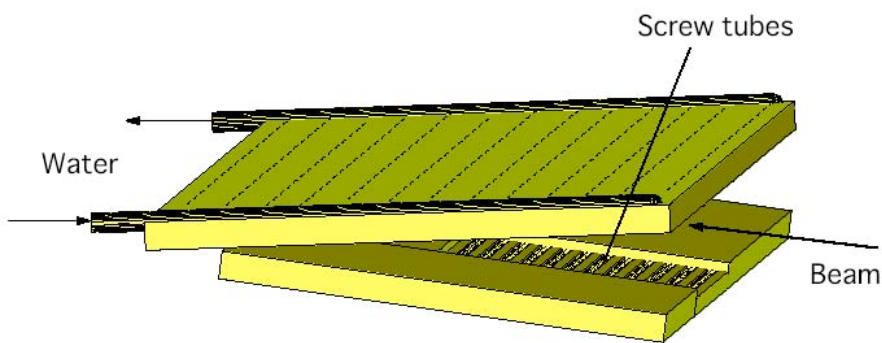


Fig. 16. A schematic diagram of the exit beam dump. It is made of copper alloy and the cooling water flows through screw tubes.

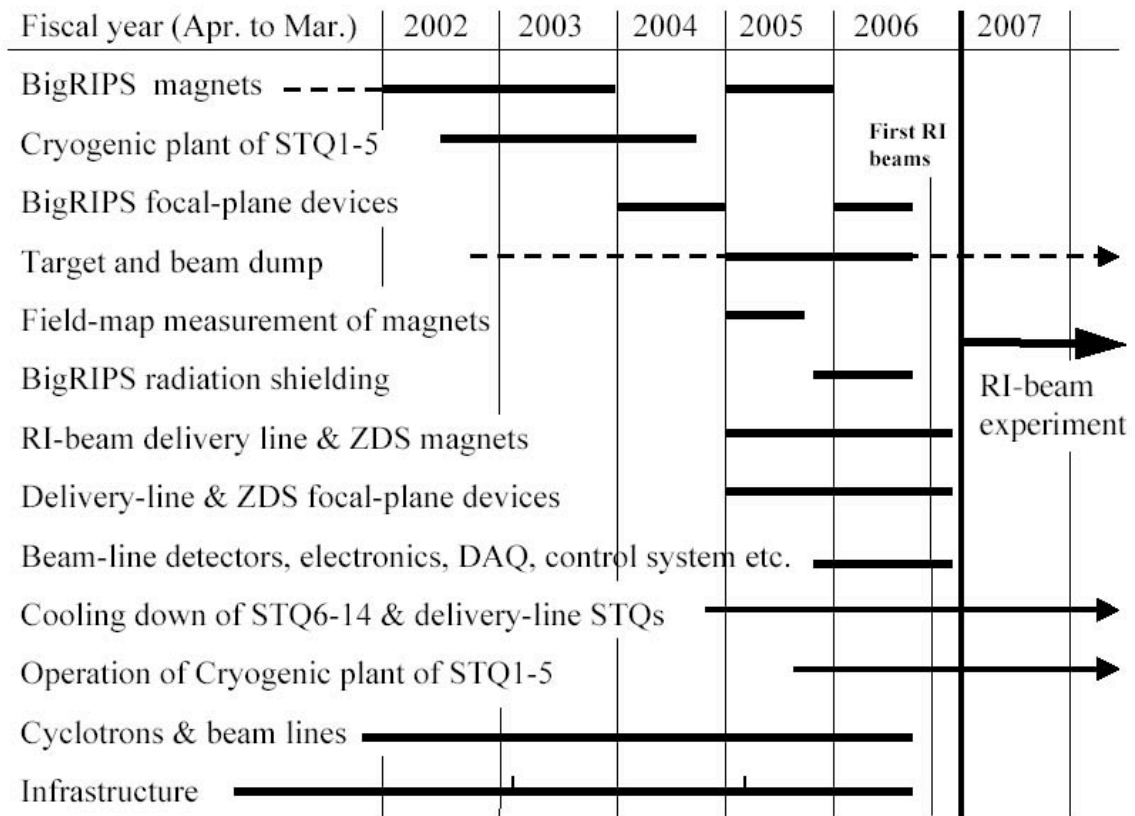


Fig. 17. Construction schedule of the BigRIPS separator project.